atmosphere

MDPI

Article

Effects of Wind Barriers on Wind Fields and Vehicle Stability on Bridges

Xiaobo Lin [1,2], Bin Lin [3], Dandan Xia [2,4,*], Li Lin [2,5,*] and Zhiqun Yuan [2,6]

1 Department of Civil Engineering, Fuzhou University, Fuzhou 350108, China; 210510010@fzu.edu.cn
2 Fujian Provincial Key Laboratory of Wind Disaster and Wind Engineering, Xiamen 361024, China; zqyuan@xmut.edu.cn
3 CCCC Second Highway Consultants Co., Ltd., Wuhan 430056, China; linbin7758@outlook.com
4 Industrial Systems Engineering, University of Regina, Regina, SK S4S0A2, Canada
5 Department of Civil Engineering and Architecture, Xiamen University of Technology, Xiamen 361024, China
6 School of Mechanical and Automotive Engineering, Xiamen University of Technology, Xiamen 361024, China
* Correspondence: xia229@uregina.ca (D.X.); 2011110904@xmut.edu.cn (L.L.)

Abstract: To explore the influence of bridge wind barriers, with their specific opening shapes and arrangements, on bridge deck wind fields and vehicle driving stability under different crosswinds, five bridge wind barrier schemes were designed. For two incoming wind speeds, the wind speed at different heights over three traffic lanes and the aerodynamic six-component force of the vehicle model were measured, and the influence of the wind barrier parameters on the vehicle driving stability was analyzed. The equivalent wind speed reduction coefficient of the wind barrier was compared with the dimensionless coefficients of the aerodynamic side force, roll moment, and aerodynamic lift to verify the accuracy of the shielding effect evaluation indices. The final conclusions provide a useful reference for designing bridge wind barriers.

Keywords: wind tunnel test; wind barrier; parameter; driving stability

check for updates

Citation: Lin, X.; Lin, B.; Xia, D.; Lin, L.; Yuan, Z. Effects of Wind Barriers on Wind Fields and Vehicle Stability on Bridges. *Atmosphere* **2022**, *13*, 318. https://doi.org/10.3390/atmos13020318

Academic Editors: Qiusheng Li, Junyi He, Bin Lu and Pak-Wai Chan

Received: 13 December 2021
Accepted: 11 February 2022
Published: 14 February 2022

Publisher's Note: MDPI stays neutral with regard to jurisdictional claims in published maps and institutional affiliations.

Copyright: © 2022 by the authors. Licensee MDPI, Basel, Switzerland. This article is an open access article distributed under the terms and conditions of the Creative Commons Attribution (CC BY) license (https://creativecommons.org/licenses/by/4.0/).

1. Introduction

As bridge spans have increased, the impact of wind loads on bridge structures and the safety of vehicles passing over bridges have received more attention from engineers [1]. This is especially important in coastal areas with extreme weather conditions [2–4]. Vehicles with a higher center of gravity are more likely to roll over when there are strong crosswinds over a bridge [5,6], and the safety of vehicles passing over bridges is important [7,8].

Many scholars have investigated the effects of vehicular types and lanes on the aerodynamic coefficients of vehicles, and the effect of aerodynamic interference on the dynamic responses of road vehicles and bridges under crosswinds [9–11]. At present, installing wind-shielding structures on both sides of a bridge is the most effective method for reducing the impact of crosswinds on vehicles traveling over bridges. However, these studies mainly focused on the aerodynamic characteristics without considerations of the protection effect of the wind barriers installed on the bridge deck. Recently, through wind tunnel tests, many scholars have studied the effect of crosswind on vehicle stability on bridges, and they have found that railings and wind barriers can effectively improve vehicle stability [12–16]. However, these studies did not investigate the impact of wind barriers with different opening shapes on vehicle stability.

In addition to protecting vehicles from adverse crosswind effects, wind barriers may adversely affect the bridge's dynamic stability. The bridge decks with wind barriers are more resilient to flutter in more turbulent winds [17]. Therefore, many researchers have used wind tunnel experiments to study the influence of the height and porosity of wind barriers on the wind resistance, and most of them used the wind speed reduction coefficient to evaluate the effect of each parameter on the wind resistance. These researchers concluded

that a wind barrier with 30% porosity and a height of 5 m provided the best wind-shielding effect, and that the hole size has little effect on wind barrier efficiency [18–22].

Recent research has mainly focused on the influence of the bridge wind barrier height, porosity, and other parameters on the wind speed shielding efficiency of bridges, while the influence of the wind barrier opening shape and arrangement on the wind field over bridges has received less attention. In addition, crosswinds act directly on vehicles on bridges. Whether the influence of the wind barrier parameters on vehicle stability on bridges is consistent with the evaluation results of the equivalent wind speed reduction coefficient on the bridge remains to be studied. Therefore, a study on the influence of the shape and arrangement of bridge wind barrier openings on wind fields over bridges and moving vehicle stability was carried out, and the results of speed tests and vehicle side force tests were compared to verify the equivalent reduction in wind speed. The coefficient was consistent with the vehicle aerodynamic evaluation index.

2. Test Model

The model was geometrically similar to the actual size, and the processing size error was within 2%. The model was made of materials with higher stiffnesses to ensure that the model had sufficient stiffness to avoid large vibrations during the test process, which could affect the accuracy [23].

2.1. Model Installation Platform

The bridge wind barrier and vehicle model were installed on a uniform box girder platform. The platform had three lanes, as shown in Figure 1. The geometric scale ratio of the bridge model was selected based on the influence of the blocking ratio ζ [23], which was calculated as:

$$\zeta = \frac{A_c}{A_m} \tag{1}$$

where A_m is the cross-sectional area of the wind tunnel and A_c is the maximum projected area of the test model on the cross-section of the test region.

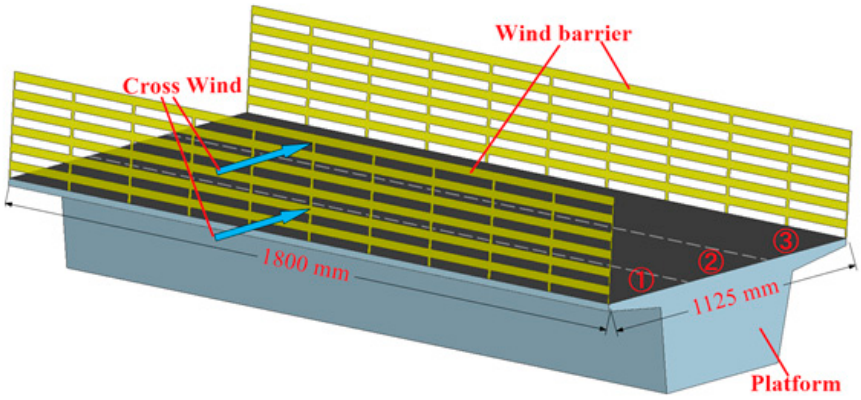


Figure 1. Model platform.

The geometric scale ratio of the model was set to 1:10, and the maximum blocking rate of the model placed in the test section was 3.75%, which satisfied the test requirement that the maximum block rate be less than 5% [23].

2.2. Wind Barrier Model

The shape and arrangement of the holes were the main model parameters. The wind tunnel tests showed that the efficiency of a wind barrier with 50% porosity was high without significantly reducing the aerodynamic stability of the bridge [24]. Therefore, a model with four different opening shapes, a porosity of 50%, and a height of 30 cm was used, and segment models are as shown in Figure 2.

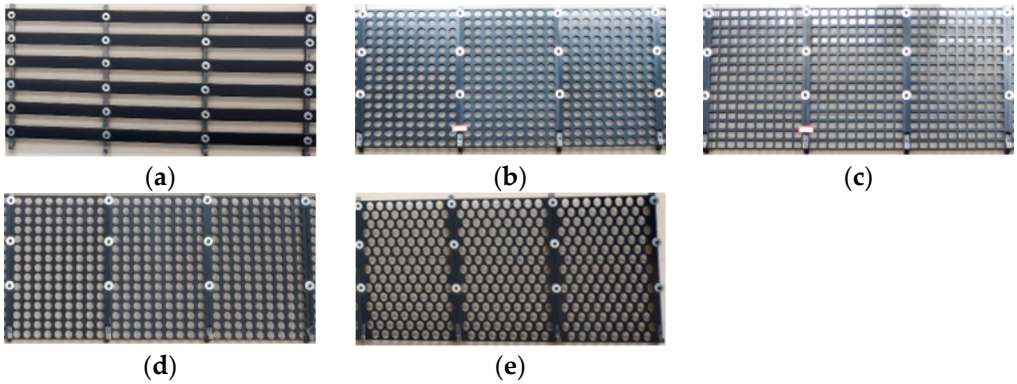


Figure 2. Segment models of wind barrier: (**a**) barrier strips; (**b**) round holes; (**c**) square holes; (**d**) elliptical holes in an equidistant arrangement; (**e**) elliptical holes in a staggered arrangement.

2.3. Vehicle Model

When they encounter lateral crosswinds, vehicles on bridges are prone to side slips, and large vehicles, such as trucks, might roll over or experience other severe accidents. In this work, a truck model was designed and fabricated for the wind tunnel tests. The truck model was made of resin, and the geometric model used a scale ratio of 1:10, which was consistent with the box girder and bridge wind barrier, as shown in Figure 3.

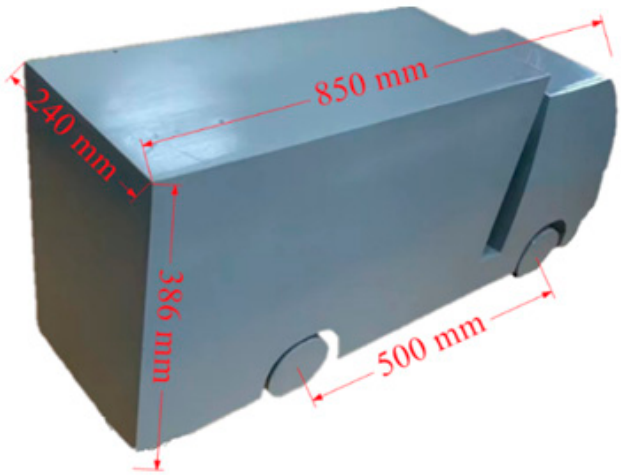


Figure 3. Truck model.

3. Test Setup

3.1. Test Conditions

Both the force test and the speed test were performed in the XMUT-WT wind tunnel at the Xiamen University of Technology. The wind tunnel had a width of 6 m, a height of 3.6 m, and a length of 25 m. The wind speed range of the empty wind tunnel was 0.5–30 m·s^{-1}, and the unevenness of the flow field was less than 1.5%. Both the force test and the speed test were performed with uniform flow fields. Two wind speeds, 7.91 m·s^{-1} and 11.07 m·s^{-1}, were selected to study the influence of the wind speed on the wind barrier efficiency and driving stability.

3.2. Measurement Positions

The sensors used in the vehicle force test were the TFI Cobra Probe pulsation anemometer (Series 100) and the ATI six-component balance (SI-130-10), and the parameters are shown in Table 1.

Table 1. Parameters of the main sensors.

Name	Place of Production	Model	Range		Accuracy
TFI Cobra Probe pulsation anemometer	Australia	Series 100	v/2–100 m·s^{-1}		±0.5 m·s^{-1}
ATI six-component balance	America	SI-130-10	F_x,F_y/(±N) F_z/(±N) T_x,T_y/(±N·m) T_z/(±N·m)	130 400 10 10	±0.025 N ±0.05 N ±0.00125 N·m ±0.00125 N·m

In the speed test, the TFI Cobra three-dimensional pulsating anemometer was used to measure the height of the vehicle model near the centerlines of lanes ①, ②, and ③; that is, the wind speed profile at a height of 0–45 cm. The intervals between the measurement points, the sampling frequency, and the duration were 2.5 cm, 600 Hz, and 60 s, respectively. Figure 4 shows the layout of the measurement points.

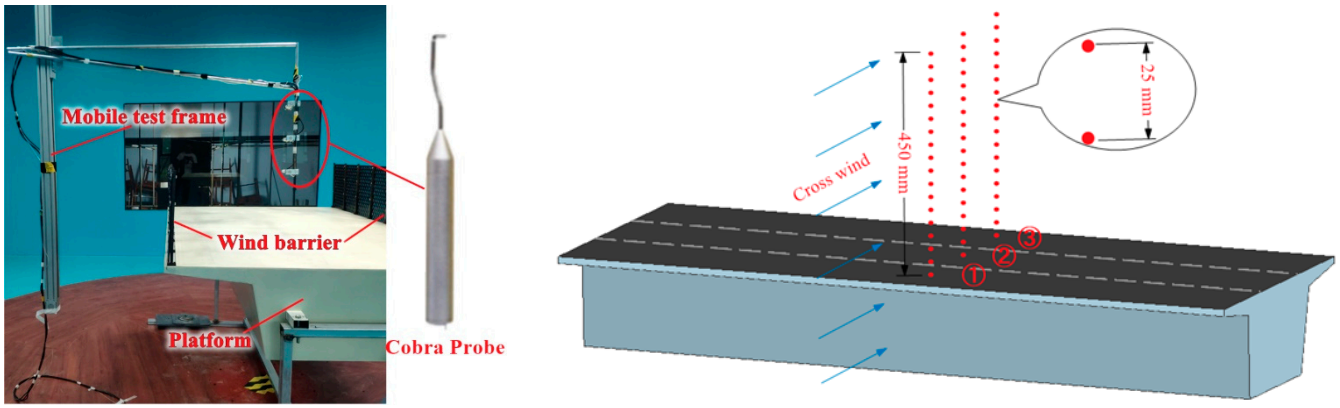


Figure 4. Layout of measurement points for the speed test.

The vehicle model was placed in lane ② on the bridge. The distance between the wheel and the bridge surface was 2 mm, and there was no error due to the contact between them. The truck was connected to a six-component balancer through a custom pole, as shown in Figure 5.

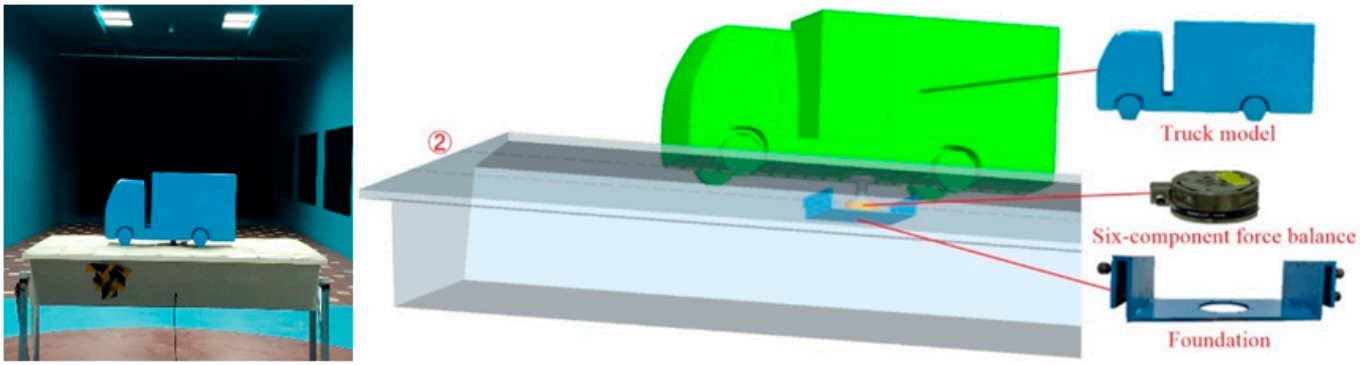


Figure 5. Schematic diagram of the model installation.

4. Analysis of Test Results

4.1. Influence of Wind Barrier Parameters on the Average Wind Profile

At the end of the test, the average wind speed at each measurement point was determined in the height direction, which gives the average wind speed profile within the height range of 0~450 mm above the centerline of each lane. These profiles can be used to analyze the impact of the parameters on the wind fields over the bridge.

(1) The arrangement of the holes

Figure 6 shows the average wind speed profiles of each lane for the three wind barrier conditions (no wind barrier, behind the wind barrier of the staggered arrangement, and behind the wind barrier of the equidistant arrangement) at two wind speeds. Figure 6 reveals that the average wind speed at each measurement point increased as the incoming wind speed increased. Under different wind speed conditions, the wind speed behind the wind barrier had the same reduction trend for different hole arrangements; that is, the shielding effect of the hole arrangement on the lanes behind the wind barrier did not change significantly with increases in the incoming wind speed. In Lane 1, the holes were arranged equidistantly, and the corresponding wind speed in the height range of 0 to 35 cm was lower than that in the staggered arrangement. The wind shield effect of the equidistant arrangement on Lane 1 was better than that of the staggered arrangement. In Lane 2 and Lane 3, there were no significant differences in the wind shield effect of the equidistant and staggered arrangements. In the most unfavorable situation, the wind shield effect of the equidistant hole arrangement was better than that of the staggered arrangement. In general, the hole arrangement does not have a significant impact on the wind shield effect of the wind barrier. Because the equidistant hole arrangement slightly improved the wind shield effect of the wind barrier, and because its production and processing are relatively simple, the remainder of the schemes were carried out with a uniformly distributed arrangement.

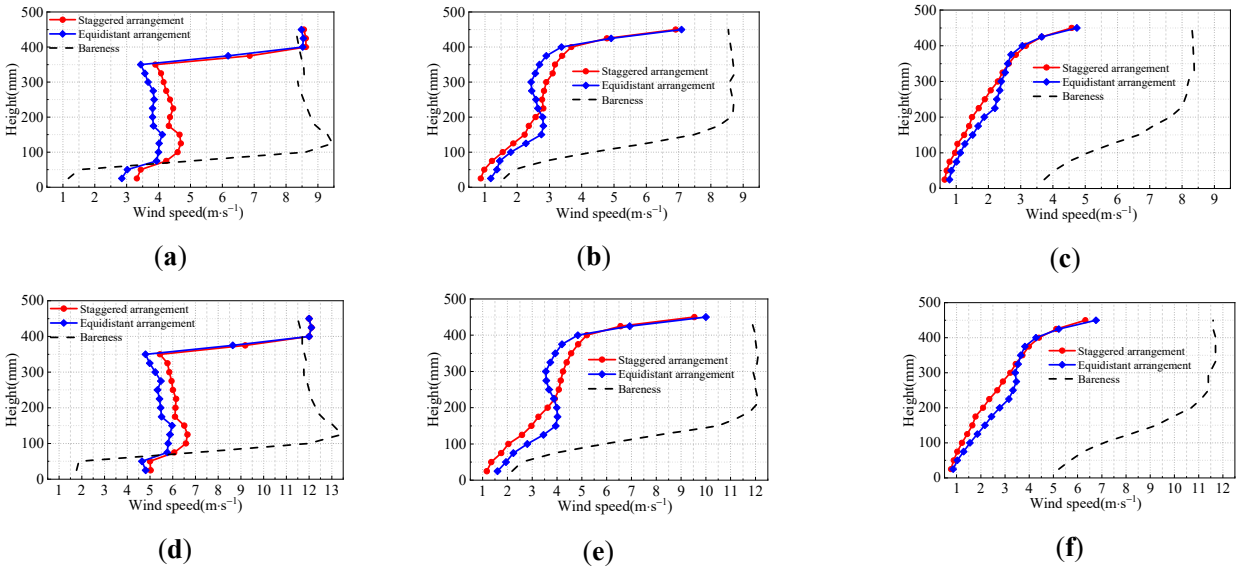


Figure 6. Comparison of wind speed reduction coefficients for each lane with different hole arrangements under two wind speed conditions: (**a**–**c**) are the data of lane 1, lane 2, and lane 3 under the condition of 7.91 m·s^{-1}, respectively; (**d**–**f**) are the data of lane 1, lane 2, and lane 3 under the condition of 11.06 m·s^{-1}, respectively.

(2) The shape of the holes

Figure 7 shows the average wind speed profile of each lane with no wind barriers, and with wind barriers that had barrier strips, round holes, elliptical holes, and square holes. The average wind speed at each measurement point increased as the incoming wind speed increased. Under different wind speed conditions, the wind speed behind the wind barriers with differently shaped holes decreased with the same trend. The wind speed has no discernable influence on the blocking effect of wind barriers with differently shaped holes. The barrier strip scheme, which is the main Chinese standard [25], is also the most commonly used perforation scheme. Although the wind speed of the barrier strip scheme in the height range of 15 cm to 30 cm was lower than that of the other schemes, the wind speed of the barrier strip scheme in the height range of 15 cm above the ground was

greater than that of the other schemes. In particular, in the barrier strip scheme, the wind speed at 10 cm above Lane 1 and Lane 2 was greater than or close to the wind speed of the corresponding measurement point under the bare bridge condition, increasing vehicle lift on the bridge surface and reducing the vehicle adhesion force of the steering wheel. This condition might cause the steering wheel to lose steering force and the driving wheel to lose traction force, which affects the steering stability of the car. The effective shielding heights above Lane 1, Lane 2, and Lane 3 of each scheme were similar, at 35 cm, 40 cm, and 40 cm, respectively. The circular hole scheme effectively shields the area by reducing the wind speed and improving the shielding effect.

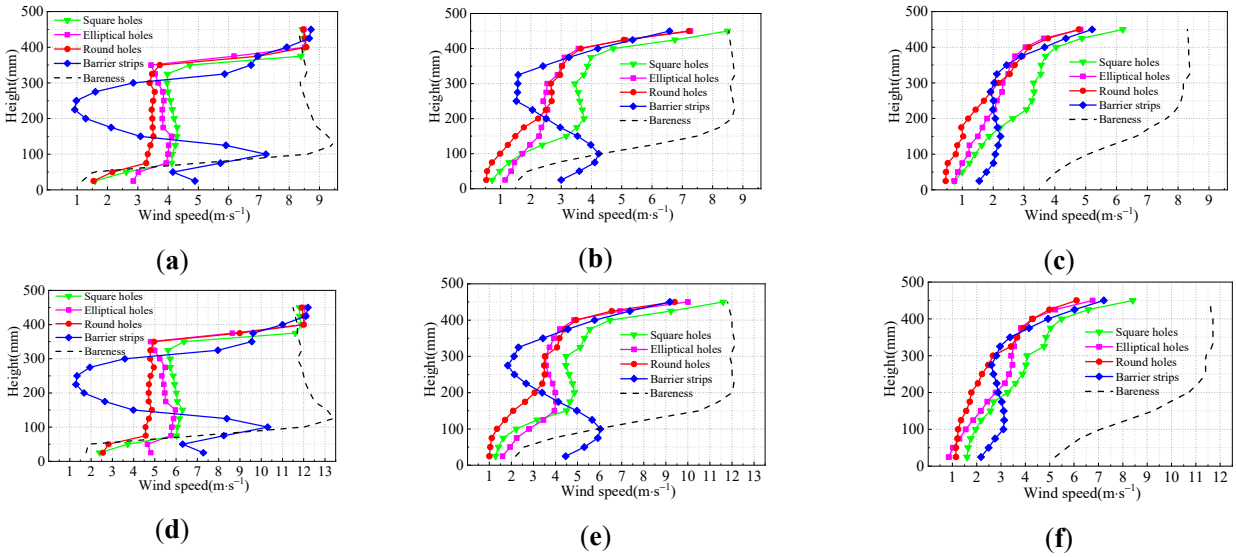


Figure 7. Comparison of wind speed reduction coefficients for each lane with different hole shape schemes under two wind speed conditions: (**a**–**c**) are the data of lane 1, lane 2, and lane 3 under the condition of 7.91 m·s^{-1}, respectively; (**d**–**f**) are the data of lane 1, lane 2, and lane 3 under the condition of 11.06 m·s^{-1}, respectively.

4.2. Analysis of the Influence of the Wind Barrier Parameters on the Wind Choke Efficiency

The wind speed reduction coefficient of each lane can be calculated with Equation (2) [26].

$$r = \sqrt{\frac{1}{z_r}\int_0^{z_r} (u(z)/u_0)^2 dz} \quad (2)$$

where Z_r is the height range of the bridge wind profile, with Z_r = 45 cm because the height of a vehicle on the bridge is usually less than 4.5 m; $u(z)$ is the transverse wind speed at height Z; and u_0 is the incoming wind speed. The smaller the wind speed reduction coefficient is, the better the wind-shielding effect of the wind barrier. Therefore, the wind-shielding effect of different bridge wind barrier schemes can be evaluated by using Equation (2).

Figure 8 shows a comparison of the reduction factor of different wind barriers under two different wind conditions of 7.91 m·s^{-1} and 11.06 m·s^{-1}.

Figure 8 shows that a wind barrier with round holes has the best wind shielding efficiency, followed by a wind barrier with elliptical holes. The barrier strip and the plate barrier with holes have their own advantages and disadvantages in each lane. In Lane 1, the plate barrier with holes performs slightly better, while the barrier strip performs slightly better in Lanes 2 and 3. The wind speed for all barriers was significantly higher in Lane 1 than in Lane 2. The wind speed was unevenly distributed in each lane. The current vehicle control issues on the bridge deck in windy conditions occur mainly when the bridge deck wind speed reaches 25 m·s^{-1}. This wind speed not only increases the probability of unfavorable situations in which the vehicle's lateral force changes excessively and reduces

vehicle stability when changing lanes, but also easily leads to excessive wind speeds on the windward side lanes. To improve the bridge wind barrier, the boundary of the windward lane should be maintained at an appropriate distance from the wind barrier.

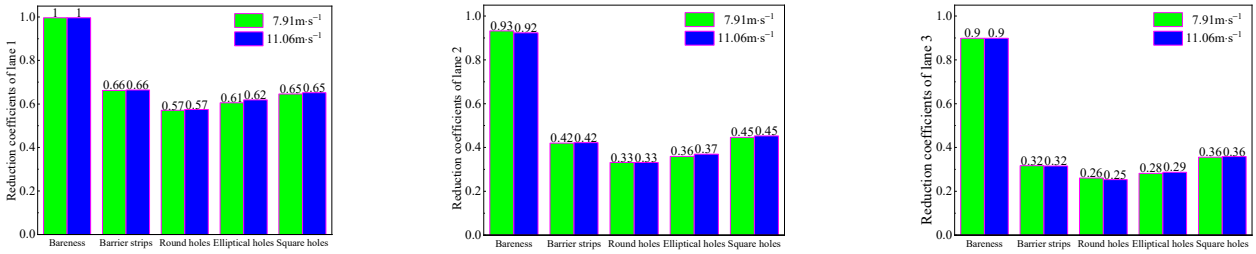


Figure 8. Comparison of wind speed reduction coefficients for each lane with different hole shape schemes under two wind speed conditions.

4.3. Influence of the Wind Barrier Parameters on Driving Stability over Bridges

The measured data were obtained from the six-component force sensor used with the truck model. According to the J1594 standard issued by the SAE Road Vehicle Aerodynamics Committee [27], the aerodynamic coordinate system can be determined by the right-hand rule, as shown in Figure 9.

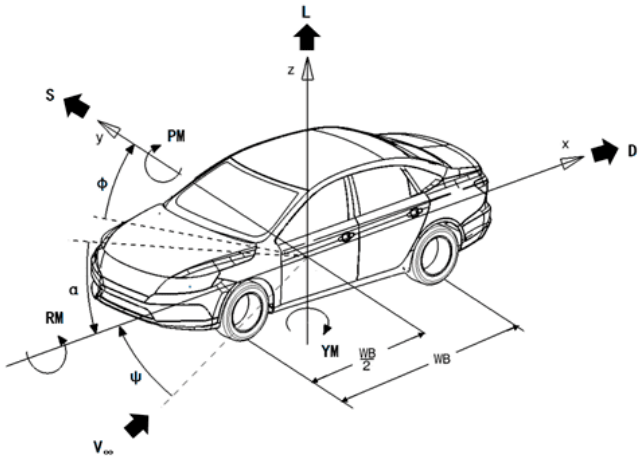


Figure 9. Automobile aerodynamics coordinate system.

With crosswinds, the aerodynamic side force, aerodynamic lift, and roll moment are important factors for vehicle stability [28]. Therefore, the aerodynamic side force, roll moment, and aerodynamic lift data obtained in the force tests were converted into the average value of the vehicle aerodynamic coordinate system, and then plotted and analyzed.

(1) The efficiency of wind barriers with different arrangements

The results from the side force tests of the truck behind wind barriers with different hole arrangements are shown in Figure 10.

Figure 10 shows that different arrangement schemes can greatly reduce the lateral force and roll moment of the truck. Although the equidistant arrangement can improve the safety of trucks traveling over bridges to a certain extent, its value is not considerably different from the scheme using the staggered arrangement, which shows that the hole arrangement has little effect. In addition, the wind barrier roll moment and lift values were smaller in the equidistant arrangement; therefore, the equidistant arrangement is beneficial to the stability of trucks driving over bridges, which is consistent with the wind test results.

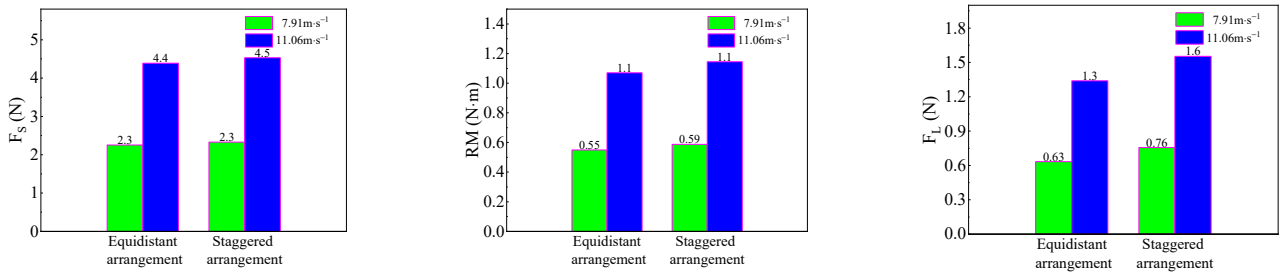


Figure 10. Comparison of the lateral force, roll moment, and lift of freight cars with different arrangement schemes under two wind speed conditions.

(2) Shielding efficiency of wind barriers with different hole shapes

Figure 11 shows the results of the truck load tests behind wind barriers with the following openings: barrier strips, round holes, elliptical holes, and square holes.

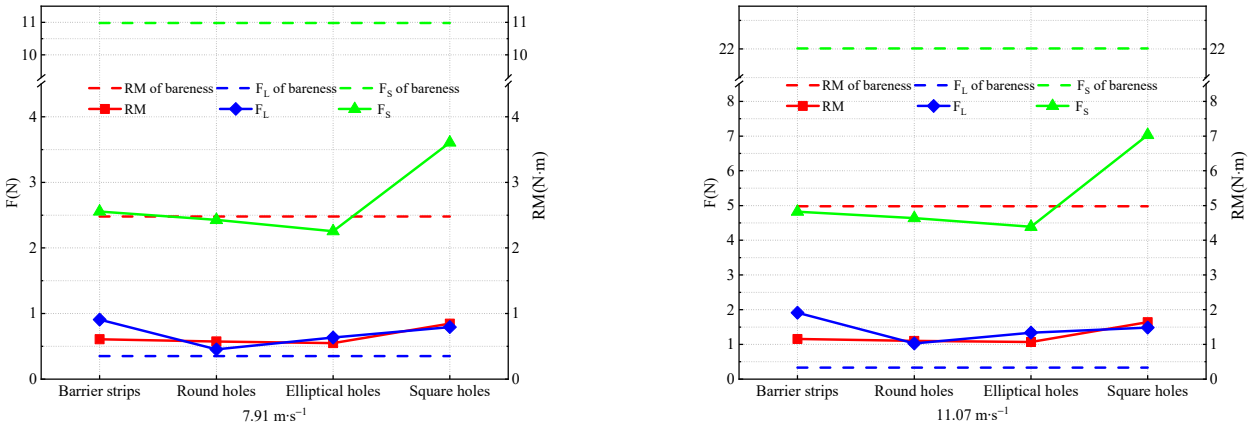


Figure 11. Comparison of the lateral force, roll moment, and lift of freight cars behind barriers with different hole shapes under two wind speed conditions.

Figure 11 shows that the installation of wind barriers can effectively reduce the aerodynamic force and roll moment of the model truck; however, the phenomenon that the aerodynamic lift of the model is greater than that of the bare bridge was due to the impact of the wind barrier on the wind within the height of the structure. The field shielding effect was improved, but the shielding effect on the top of the model was poor due to the large pressure difference between the upper and lower sides of the vehicle model. Therefore, when evaluating the performance of the wind barrier, it is necessary to consider the impact of the pressure difference at different heights of the bridge deck wind fields on the aerodynamic lift of the vehicle. Overall, the wind barrier with circular holes had the best shielding effect and increased the stability of trucks driving over bridges.

4.4. Comparison of Force Tests and Flow Field Tests Results

The main purposes of installing wind barriers on bridges are to reduce the impact of lateral crosswinds on the bridge deck and to improve the driving comfort and safety of vehicles passing over bridges in windy weather. Currently, bridge wind barriers use the bridge deck equivalent wind speed reduction coefficient as the wind shield performance evaluation index, but the influence of bridge wind barriers on vehicle stability on bridge decks is not clear. Additionally, it is unknown whether the effects of bridge wind barriers are consistent with the bridge deck equivalent wind speed reduction coefficient. Therefore, the equivalent wind speed, aerodynamic side force, overturning moment, and aerodynamic lift of the vehicle model measured for the different wind barrier schemes were divided by the test values measured under the bare bridge condition, and the corresponding dimensionless

reduction coefficients were obtained through nondimensionalization. Figure 12 shows the equivalent wind speed reduction coefficient W, aerodynamic side force reduction coefficient F_S, roll moment reduction coefficient RM, and aerodynamic lift reduction coefficient L_S for each scheme, as well as the bridge deck in the 0–4 m height range of the lane.

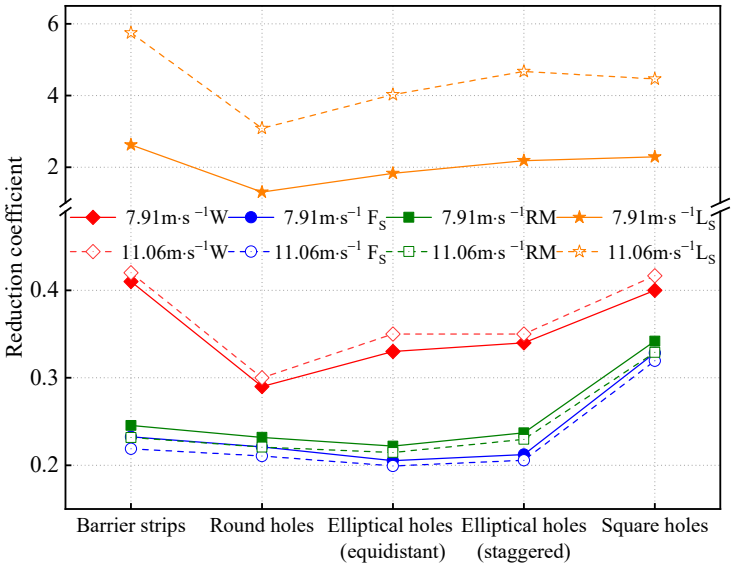


Figure 12. Comparison of reduction coefficients of each model under two wind speed conditions.

Figure 12 shows that under different wind speed conditions, the aerodynamic lift reduction coefficient of each wind barrier scheme was greater than that of the bare bridge condition; the difference increased with increasing wind speed, and the lift reduction coefficient increased by more than 100% in some cases. The lift increased because the pressure difference between the up- and downflows at the bottom of the vehicle model increased as the incoming wind speed increased, and the change in the pressure difference in the roof was small. The aerodynamic side force reduction coefficient and roll moment reduction coefficient were similar, while the equivalent wind speed reduction coefficient was larger than the aerodynamic side force reduction coefficient and the roll moment reduction coefficient. Since the measurement point in the speed test was located at the center of the two wind barrier columns, the wind barrier had a poor shielding performance; thus, the wind speed reduction coefficient was larger. In the force test, because the length of the truck was greater than the distance between the two columns of the wind barrier, the overall reduction coefficient was relatively small. It is safer to use the wind speed reduction coefficient to evaluate the wind barrier performance. Since the equivalent wind speed reduction coefficient was consistent with the lift reduction coefficient, the speed test can reflect the adverse effects of the pressure difference at different heights of the bridge wind fields on the aerodynamic lift of vehicles on bridges with wind barriers with different opening shapes. It is appropriate to use the bridge deck equivalent wind speed to evaluate the overall performance of the different wind barriers, and the speed test can measure multiple points at the same wind speed due to the side frame and multilane measurement. Future follow-up research can use this evaluation method to improve efficiency by considering the influence of pressure differences at different heights of wind fields over bridges on the aerodynamic lift of vehicles.

5. Conclusions

On the basis of wind tunnel speed tests, with force tests of wind barriers and vehicle models, where we assessed the influence of wind barrier hole arrangements and hole shapes on bridge deck wind fields and vehicle driving stability, and our comparison analysis, the following conclusions were obtained:

(1) The wind speed, aerodynamic side force, and roll moment of a vehicle behind a wind barrier on a bridge increase as the incoming wind speed increases. The aerodynamic lift can increase by up to 100%. Under different wind speed and incoming flow conditions, the change in the equivalent wind speed reduction coefficient is consistent with that of the lift reduction coefficient. The speed measurement test can reflect the adverse effects of pressure difference changes at different heights of the bridge wind fields on the aerodynamic lift of vehicles with wind barriers.
(2) The arrangement of wind barrier holes has a relatively small influence on the equivalent wind profile and vehicle six-component force measures. The equidistant grid arrangement is more effective at wind blocking than other arrangements.
(3) From high to low, the wind-shielding efficiencies of wind barriers are: slabs with round holes, slabs with elliptical holes, and slabs with rectangular holes. Near the ground level, the barrier strip scheme performs significantly better than the other schemes. The opening form adopted by the current Chinese standard [25] has blind spots for blocking, and wind barriers can be further optimized.
(4) It is more efficient to use the equivalent wind speed reduction coefficient as the evaluation index of the overall efficiency of a wind barrier.

Author Contributions: Conceptualization, X.L., B.L., D.X., L.L.; methodology, X.L., B.L., Z.Y.; formal analysis, X.L., B.L., D.X., L.L.; data curation, X.L., B.L., D.X.; writing—original draft preparation, X.L., B.L., D.X.; writing—review and editing, X.L., D.X., L.L.; project administration, L.L., Z.Y.; funding acquisition, L.L., Z.Y. All authors have read and agreed to the published version of the manuscript.

Funding: This research was funded by the Industry–University Cooperation Project of Fujian Province (2020H6022), the Natural Sciences Foundation of Fujian Province (2020J01275, 2021Y0045), the Fujian Provincial Project of Transportation Science and Technology (202022, 201903), and the Wind Engineering Service Platform of Xiamen (No. 3502Z20161016).

Institutional Review Board Statement: Not applicable.

Informed Consent Statement: Not applicable.

Conflicts of Interest: The authors declare no conflict of interest.

References

1. Liu, S.; Zhao, L.; Fang, G.; Hu, C.; Ge, Y. Investigation on aerodynamic force nonlinear evolution for a central-slotted box girder under torsional vortex-induced vibration. *J. Fluids Struct.* **2021**, *106*, 103380. [CrossRef]
2. Lin, L.; Chen, K.; Xia, D.; Wanga, H.; Hua, H.; Hea, F. Analysis on the wind characteristics under typhoon climate at the southeast coast of China. *J. Wind Eng. Ind. Aerodyn.* **2018**, *182*, 37–48. [CrossRef]
3. Xia, D.; Dai, L.; Lin, L.; Wang, H.; Hu, H. A field measurement based wind characteristics analysis of a typhoon in near-ground boundary layer. *Atmosphere* **2021**, *12*, 873. [CrossRef]
4. Kozmar, H.; Procino, L.; Borsani, A. Sheltering efficiency of wind barriers on bridges. *J. Wind. Eng. Ind. Aerodyn.* **2012**, *107–108*, 274–284. [CrossRef]
5. Yamamoto, K.; Ejiri, A.; Oya, M. Rollover prevention control of vehicles with crosswind disturbance. *Artif. Life Robot.* **2021**, *26*, 250–258. [CrossRef]
6. Baker, C.; Cheli, F.; Orellano, A.; Nicolas, P.; Carsten, P.; Rocchi, D. Cross-wind effects on road and rail vehicles. *Veh. Syst. Dyn.* **2009**, *47*, 983–1022. [CrossRef]
7. Coleman, S.A.; Baker, C.J. The Reduction of Accident Risk for High Sided Road Vehicles in Cross Winds. *J. Wind Eng. Ind. Aerodyn.* **1992**, *44*, 2685–2695. [CrossRef]
8. Buljac, A.; Kozmar, H.; Macháček, M.; Pospisil, S. Self-excited vibrations of a bridge deck with single and double wind barriers. *Lect. Notes Civ. Eng.* **2019**, *27*, 124–132.
9. Zhu, L.D.; Li, L.; Xu, Y.L. Wind tunnel investigations of aerodynamic coefficients of road vehicles on bridge deck. *J. Fluids Struct.* **2012**, *30*, 35–50. [CrossRef]
10. Dorigatti, F.; Sterling, M.; Rocchi, D.; Belloli, M. Wind tunnel measurements of crosswind loads on high sided vehicles over long span bridges. *J. Wind Eng. Ind. Aerodyn.* **2012**, *107–108*, 214–224. [CrossRef]
11. Han, Y.; Cai, C.S.; Zhang, J.; Chen, S. Effects of aerodynamic parameters on the dynamic responses of road vehicles and bridges under cross winds. *J. Wind Eng. Ind. Aerodyn.* **2014**, *134*, 78–95. [CrossRef]
12. Chen, N.; Li, Y.; Wang, B. Effects of wind barrier on the safety of vehicles driven on bridges. *J. Wind Eng. Ind. Aerodyn.* **2015**, *143*, 113–127. [CrossRef]

13. Kim, S.; Shim, J.; Kim, H. How wind affects vehicles crossing a double-deck suspension bridge. *J. Wind Eng. Ind. Aerodyn.* **2020**, *206*, 104329. [CrossRef]
14. Chu, C.; Chang, C.; Huang, C.; Chih-Jung, H.; Tso-Ren, W.; Chung-Yue, W.; Ming-Yi, L. Windbreak protection for road vehicles against crosswind. *J. Wind Eng. Ind. Aerodyn.* **2013**, *116*, 61–69. [CrossRef]
15. He, X.; Zou, S. Crosswind effects on a train-bridge system: Wind tunnel tests with a moving vehicle. *Struct. Infrastruct. Eng.* **2021**, 1–13. [CrossRef]
16. Xue, F.R.; Han, Y.; Zou, Y.F.; He, X.; Chen, S. Effects of wind-barrier parameters on dynamic responses of wind-road. *J. Wind Eng. Ind. Aerodyn.* **2020**, *206*, 104367. [CrossRef]
17. Buljac, A.; Kozmar, H.; Pospíil, S.; Macháček, M.; Kuznetsov, S. Effects of wind-barrier layout and wind turbulence on aerodynamic stability of cable-supported bridges. *J. Bridge Eng.* **2020**, *25*, 04020102. [CrossRef]
18. Li, B.; Zhang, J.; Yang, Q. Experimental study on wind-shielding performance of bridge wind barriers. *Vib. Shock* **2016**, *35*, 78–82.
19. Kozmar, H.; Procino, L.; Borsani, A. Optimizing height and porosity of roadway wind barriers for viaducts and bridges. *Eng. Struct.* **2014**, *81*, 49–61. [CrossRef]
20. Zhan, K.; Lin, X.; Yang, Y. Experimental study on bridge wind barrier performance under different structural parameters. *J. Fuzhou Univ.* **2021**, *49*, 217–224.
21. Lin, X.; Hou, H.; Lian, J. Analysis on the influence parameters of wind barrier performance of double beam bridges. *J. Fuzhou Univ.* **2021**, *49*, 87–94.
22. Su, Y.; Li, Y.; Peng, D.; Chen, K.; Meng, X. Wind tunnel test study of full-scale model of highway wind barrier flow field characteristics and its own wind load. *Eng. Mech.* **2017**, *34*, 87–94.
23. Ge, Y. *Bridge Wind Tunnel Test Guide*; China Communications Press: Beijing, China, 2018.
24. Wei, G. *Research on Numerical Methods of Safety Countermeasures for Side Wind driving on Highways and Bridges*; Chang'an University: Xi'an, China, 2013.
25. China MOT. *Wind Barrier for Bridges*; China Communications Press: Beijing, China, 2013.
26. Zhou, Q.; Zhu, L.; Guo, Z. Numerical simulation for curve windshield barrier effects on wind environment around bridge deck. *J. Wuhan Univ. Technol.* **2010**, *32*, 38–44.
27. Yu, Z. *Automobile Theory*; Mechanical Industry Press: Beijing, China, 2000.
28. Wang, F.; Fu, L.; Hu, X. Transient numerical simulation of the influence of different intensities of crosswinds on car aerodynamic characteristics. *J. Jilin Univ.* **2008**, *38*, 19–22.